

Recalculation of 23 mouse HDL QTL datasets improves accuracy and allows for better candidate gene analysis

Cheryl Ackert-Bicknell, Beverly Paigen, and Ron Korstanje¹

The Jackson Laboratory, Bar Harbor, ME

Abstract In the past 15 years, the quantitative trait locus (QTL) mapping approach has been applied to crosses between different inbred mouse strains to identify genetic loci associated with plasma HDL cholesterol levels. Although successful, a disadvantage of this method is low mapping resolution, as often several hundred candidate genes fall within the confidence interval for each locus. Methods have been developed to narrow these loci by combining the data from the different crosses, but they rely on the accurate mapping of the QTL and the treatment of the data in a consistent manner. We collected 23 raw datasets used for the mapping of previously published HDL QTL and reanalyzed the data from each cross using a consistent method and the latest mouse genetic map. By utilizing this approach, we identified novel QTL and QTL that were mapped to the wrong part of chromosomes. Our new HDL QTL map allows for reliable combining of QTL data and candidate gene analysis, which we demonstrate by identifying *Grin3a* and *Etv6*, as candidate genes for QTL on chromosomes 4 and 6, respectively. In addition, we were able to narrow a QTL on Chr 19 to five candidates.—Ackert-Bicknell, C., B. Paigen, and R. Korstanje. Recalculation of 23 mouse HDL QTL datasets improves accuracy and allows for better candidate gene analysis. *J. Lipid Res.* 2013. 54: 984–994.

Supplementary key words high-density lipoprotein • quantitative trait locus • meta-analysis

In the past decade, high-density lipoprotein (HDL) cholesterol has emerged as a new potential therapeutic target for the treatment of cardiovascular disease (CVD). The key role of HDL as a carrier of excess cellular cholesterol in the reverse cholesterol transport pathway is believed to provide protection against atherosclerosis (1). Several epidemiologic studies have demonstrated that HDL is a strong inverse predictor of CVD risk (2–5). Although much is known about HDL metabolism and reverse cholesterol transport, we still do not have a complete understanding of all the genetic factors involved in the regulation of HDL levels. Also, HDL is not a single entity but can be subdivided into different subpopulations. The relationships

among these different subpopulations are not understood, and the genes responsible for the subpopulation differences among individuals are unknown.

Several approaches, including genetic mapping studies, have been used to identify novel genes involved in the regulation of HDL levels. In mice, the technique of quantitative trait locus (QTL) mapping, which uses crosses between different inbred strains of mice, has been heavily employed over the past 15 years. These results have been summarized in several reviews (6, 7). One limitation of traditional QTL analysis is low mapping resolution, which is a result of the limited genetic recombination possible in one-generation backcrosses [i.e., $A \times (A \times B)$] and two-generation intercrosses [i.e., $(A \times B) \times (A \times B)$]. The 95% confidence interval (CI), the interval in which the causative gene is most likely to reside, is usually very broad. For example, one large study of bone mineral density QTL found that the average CI width for traditionally mapped QTL was 32 cM (8). As it can be assumed that there are, on average, 20 genes per cM (9), the number of candidate genes per QTL can be very large, making the identification of the causative gene very difficult. In the past few years, several methods have been developed that combine accumulated data from the different crosses, allowing for narrowing of the CI for QTL and reducing candidate gene lists (10). However, the success of these methods heavily depends on the accuracy of the QTL mapping.

The current standard genetic map for the mouse is curated and maintained by the Mouse Genome Informatics (MGI) Group at The Jackson Laboratory (www.informatics.jax.org) (11). Mapping QTL requires accurate genetic map information for both the relative order of markers and the distances between them (12). Recently, Shifman and colleagues published a new genetic map based on a large population of a heterogeneous stock (13). Cox and colleagues integrated a total of 7,080 standard, simple-sequence length polymorphism (SSLP) markers to this single-nucleotide polymorphism (SNP)-based map, generating a corrected mouse genetic map (14). This new map

This work was supported by the National Institutes of Health Grants R01 HL-077796, R01 HL-081162, R01 HL-095668, and R01 AR-060234.

Manuscript received 10 October 2012 and in revised form 6 February 2013.

Published, JLR Papers in Press, February 7, 2013

DOI 10.1194/jlr.M033035

Abbreviations: Chr, chromosome; LOD, logarithm of the odds; MGI, Mouse Genome Informatics; QTL, quantitative trait locus; SNP, single-nucleotide polymorphism.

¹To whom correspondence should be addressed.

e-mail: ron.korstanje@jax.org

Copyright © 2013 by the American Society for Biochemistry and Molecular Biology, Inc.

resolved inconsistencies between the physical and genetic maps and is now the standard MGI genetic map, providing highly accurate genetic distances. A recent mapping study, in which the new and traditional genetic maps were compared, suggests that up to 20% of published QTL may have been mislocalized due to marker order and positioning errors in the old genetic map (14).

In addition, many advances have been made over the years in the statistics and insights underlying QTL mapping. For example, in the past, males and females were analyzed as one population, disregarding possible sex-associated differences in the phenotype, or as two separate populations, resulting in a loss of power. We now analyze males and females as one population, using sex as a covariate. This method results in higher power compared with analyzing them separately, and it takes into account the obvious differences between males and females. Another issue is the direction of the cross. While, for most crosses, all F1 animals were produced by crossing a female from strain A with a male from strain B, in some crosses, the F1 animals originated from reciprocal crosses (A×B and B×A) and the F2 progeny were analyzed regardless of the parental grandmother. Now that we are aware of the epigenetic differences that can occur depending on the direction of the cross, we use the paternal grandmother as a covariate when analyzing the data (12).

The different HDL QTL datasets have been analyzed in various ways using different genetic maps and often without the above-mentioned covariates. This has resulted in misplaced QTL, missed QTL, or QTL that were only suggestive because of the loss of power. In this study, we made a concerted effort to identify and collect as many published, historical HDL QTL datasets as possible and reanalyze them. While most of the data used in this study were generated by our research group, several datasets were kindly provided by other investigators. All data underwent rigorous quality control and were then analyzed using current statistical methods. In all cases, the new corrected genetic mouse map was used. By analyzing the different datasets in the same way and by using the same genetic map, we created a more consistent and complete mouse HDL QTL map. As we demonstrate in our study, this improved map will aid in the search for novel HDL genes.

METHODS

Identification of mapping-cross datasets

First, a literature search to identify published reports of mouse HDL QTL was done using the following key words: “HDL,” “QTL,” and “mouse.” Second, the Mouse Genome Informatics Database (www.informatics.jax.org/) was searched for HDL QTL using the Genes and Markers Query form. Specifically, this database was searched using the keyword “HDL” in the Gene/Marker Symbol/Name field, “QTL” in the Type field, and “Any” in the ‘Chromosome field; the No Limit box was checked under the heading of Maximum Returned. The cross in which each HDL QTL was mapped was identified and compared with the list of crosses identified by conventional literature search. In short, the result was a list of mouse mapping crosses in which HDL QTL were mapped regardless of the method used to measure HDL.

Main-effects QTL mapping

Map positions for the markers for all datasets were updated to the new mouse genetic map using a mouse map converter tool (<http://cgd.jax.org>). All QTL analyses were done using the R/ qtl software package (12) (R Version 2.6.2, qtl Library Version 1.09-43, www.rqtl.org/). Data were examined for phenotypic outliers and for genotyping errors, as previously described (8). A single locus main-scan for QTL was performed, and LOD scores were calculated at 2 cM intervals across the genome using the EM (or expectation-maximization) method in R/qtl for all datasets. The LOD thresholds for significant and suggestive QTL were determined in a cross-specific manner based on 1,000 permutations of the data. A QTL was considered to be suggestive if the LOD score exceeded the $P < 0.63$ threshold and significant if it exceeded the $P < 0.05$ threshold. These thresholds were chosen because they are the widely accepted cutoffs for suggestive and significant QTL.

For 5 of the 23 crosses, data were available for both male and female mice (Table 1). To account for the average differences between the males and females, we carried out scans using sex as an additive covariate. To identify sex-dependent QTL effects, we carried out additional scans using sex as an interactive covariate and computed the differences in LOD scores between these two scans (i.e., the Δ LOD) (12). The interactive scan model identified the most likely position of the sex-specific QTL. Calculating the Δ LOD score at the peak position is the secondary test for the QTL-by-sex interaction. This secondary test is carried out with no adjustment for multiple testing, and the threshold, based on the usual chi-square distribution of the likelihood ratio, is 2.0 on the LOD scale. However, sex specificity of QTL was not confirmed by further analysis, and thus all “sex-specificity” of QTL should be considered putative. For 6 of the 23 crosses, data were available for two different cross directions (i.e., B×A and A×B, Table 1). Putative cross-direction-specific QTL were identified using the strain of paternal grandmother (pgm) for each mouse as both an additive and interactive covariate, as was done for sex-specific QTL. In only one cross, both males and females were examined in crosses generated in a reciprocal fashion. In this last dataset, the interactive term of sex:pgm was examined to identify QTL that interacted with sex and were cross-direction specific; no such QTL, however, were identified in this study.

Resequencing of SNPs

High-quality genomic DNA from the different inbred mouse strains was obtained from the Jackson Laboratory’s DNA Resource (www.jax.org/dnares/). Primers were designed spanning the exon that contained the SNP and ordered from Integrated DNA Technologies. PCR and Sanger sequencing were performed using standard protocols. Sequence data were analyzed using Sequencher 4.9.

RESULTS

Datasets used in this study

From our literature search, we determined that 28 datasets would be of interest to us for this project. However, 5 of these datasets were no longer available due to loss of records or the inability to contact the lead authors. In sum, we obtained a total of 23 independent datasets (summarized in Table 1). Of these datasets, 19 were from our own laboratory. Of the remaining 4 datasets, 2 were kindly provided by Drs. Breslow and Lusic, respectively (15, 16), and the other two were obtained from the QTL archive

TABLE 1. Description of the cross datasets

Cross	Year (Reference)	Number (Sex)	Direct ^a	Age (Weeks)	Notes on Diet
(NZB×SM)NZB	2002 (40)	90 (F)	Uni	8, 12, 16, 26	Chow diet first 8 weeks, followed by atherogenic diet for 18 weeks
D2×CAST	2003 (41)	278 (M)	Bi	16	Chow diet first 8 weeks, followed by atherogenic diet for 8 weeks
B6×CASA	2003 (15)	184 (F) 185 (M)	Uni	11	Chow diet
B6×D2	2003 (16)	111 (F)	Uni	52, 68	Chow diet first 52 weeks, followed by atherogenic diet for 16 weeks
(B6×NZB)B6	2003 (42)	100 (F)	Uni	8, 12, 23	Chow diet first 8 weeks, followed by atherogenic diet for 15 weeks
SM×NZB	2004 (43)	259 (F) 254 (M)	Uni	8, 14, 20, 24	Chow diet first 8 weeks, followed by atherogenic diet for 16 weeks
B6×129S1	2004 (44)	294 (F)	Uni	20	Chow diet first 6 weeks, followed by atherogenic diet for 14 weeks
129S1×CAST	2004 (45)	277 (M)	Bi	16	Chow diet first 8 weeks, followed by atherogenic diet for 8 weeks
RIII×129S1	2004 (46)	150 (M) 180 (M)	Bi	16 20	Chow diet first 8 weeks, followed by atherogenic diet for 8 or 12 weeks
PERA×I	2006 (47)	164 (F) 141 (M)	Bi	16	Chow diet first 8 weeks, followed by atherogenic diet for 8 weeks
D2×PERA	2006 (47)	166 (M) 158 (M)	Bi	16	Chow diet first 8 weeks, followed by atherogenic diet for 8 weeks
B6×A	2006 (48)	343 (M)	Uni	10	Chow diet
B6×A	2006 (48)	271 (F)	Uni	8	Chow diet
NZB×RF	2007 (49)	542 (F)	Uni	10	Chow diet
D2×DU6i	2007 (50)	228 (M) 174 (F)	Uni	6	Chow diet
B6.Apoc ^{-/-} ×C3H.Apoc ^{-/-}	2008 (51)	241 (F)	Uni	18	Chow diet first 6 weeks, followed by western diet for 12 weeks
B6×C3H	2009 (52)	277 (F)	Uni	14	Chow diet first 8 weeks, followed by atherogenic diet for 6 weeks
(NZO×NON)NON	2009 (52)	204 (M)	Bi	24	Chow diet
B6×D2	2009 (52)	340 (M)	Uni	8	Chow diet
B6×129S1	2009 (19)	242 (F) 249 (M)	Uni	11, 18	Chow diet first 11 weeks, followed by atherogenic diet for 7 weeks
NOD(NOD×129.H2g7)	2009 (53)	159 (F)	Uni	40	Chow diet
B6×NOD	Unpublished	139 (M)	Uni	10	Chow diet
B6×NZW	Unpublished	143 (M)	Uni	10	Chow diet

^aUni = all F1 animals were produced using the direction as indicated in the first column, with the first strain being the female; bi = F1 animals were produced using both directions.

(www.qtlarchive.org), a free public access repository for QTL mapping datasets.

A large number of main-effects QTL were mapped

The analyses for single main effect QTL resulted in 143 QTL (Table 2, Fig. 1). In many instances, our analyses confirmed QTL that had been previously reported in the literature, but in other instances, our analyses yielded disparate results when compared with the published findings (Figs. 2, 3). For example, we observed that some QTL moved significantly on the same chromosome, the confidence interval width changed for some QTL, and peak LOD scores were different for many QTL. These dissimilarities were caused by the discrepancies between the genetic map we used and those used in the original studies (14) and because of methodological differences in the way we conducted our analyses compared with the original (8).

New HDL QTL map is required to determine the number of independent HDL QTL

As previously reported, many of the QTL comap to the same loci, suggesting a common underlying causative gene (7). The most striking example of HDL QTL clustering is observed on the distal end of Chromosome (Chr) 1 (Fig. 2). By using bioinformatics techniques, such as haplotyping,

which leverages these comapping QTL clusters, we previously showed that a single nucleotide polymorphism (SNP) in *Apoa2* is the most likely causative SNP underlying the QTL mapped to distal Chr 1 in all crosses where the two strains were polymorphic for this SNP (17). However, *Apoa2* is not the only distal Chr 1 gene to influence HDL (18). Careful examination of the QTL mapped to distal Chr 1 in this study showed three clusters of comapping QTL: one cluster of five QTL centered at 70 cM, one cluster of nine QTL centered at 80 cM, and one cluster of four QTL centered at 85 cM. The *Apoa2* gene (80 cM) is the most likely candidate for this middle cluster, whereas *Soat1* (67.7 cM) is the most likely candidate for the upper cluster (19). The gene underlying the most distal cluster remains unknown.

Grin3a is a candidate gene for an HDL QTL on mouse Chr 4

We mapped nine QTL to mouse Chr 4, including a cluster of four QTL with peak locations between 26 and 29 cM (Table 2, Fig. 3A). This QTL cluster consisted of QTL mapped in the following crosses (underlined strains indicate the high allele for each QTL): PERA×I (peak at 26 cM), B6×A (peak at 27 cM), D2×129 (peak at 27 cM), and 129×CAST (peak at 29 cM). The minimum shared interval for these QTL extended from 20 to 31 cM (38.6–56.2 Mb),

TABLE 2. Main scan QTL peaks

Chr	Peak (cM)	Interval (cM)	LOD	Sex	Age (Weeks)	Diet	High	Cross	Remark	
1	44	18-66	1.9	F (M?)	18	Ath	SM	(NZB×SM)NZB		
	45	29-76	2.2	M+F	11	Chow	CASA	B6×CASA	Add	
	63	16-74	3.2	F	10	Chow	RF	NZB×RF	Add	
	68	54-88	4.5	M (F?)	8	Chow	CAST	CAST×129S1		
	70	52-80	7.4	F (M?)	8	Chow	A	B×A		
	70	46-82	2.8	M+F	10	Chow	NOD	B6×NOD		
	70	63-88	3.9	M (F?)	8	Chow	RIII	129×RIII		
	72	62-76	5.8	M+F	16	Ath	PERA	D2×PERA		
	78	64-90	2.7	M (F?)	8	Chow	DBA	B6×D2		
	78	74-80	27.9	M+F	16	Ath	129	B6×129S1		
	80	78-80	51.2	M+F	8	Chow	129	B6×129S1		
	80	76-84	15.0	M+F	10	Chow	NZW	B6×NZW		
	80	76-82	8.8	F (M?)	40	Chow	Het	NOD×129S1		
	81	73-87	7.3	F (M?)	8	Chow	Het	(B6×NZB)B6		
	81	73-85	8.3	M+F	8	Chow	NZB	NZB×SM		
	81	71-91	4.5	M (F?)	16	Ath	RIII	129×RIII		
	82	74-88	9.8	F (M?)	14	Western	C3H	B6×C3H		
	82	66-86	6.8	F (M?)	18	Ath	C3H	B6×C3H-Apoe KO		
	84	84-90	10.6	F (M?)	20	Ath	129	B6×129S1		
	85	63-89	2.2	F (M?)	23	Ath	Het	(B6×NZB)B6		
	85	75-89	4.6	M+F	20	Ath	NZB	NZB×SM		
	85	77-91	3.0	M+F	24	Ath	NZB	NZB×SM		
	85	2-85	2.2	M (F?)	24	Chow	NON	(NON×NZO)NON		
	87	67-91	3.1	M+F	14	Ath	NZB	NZB×SM		
	89	75-89	5.6	F (M?)	23	Ath	Het	B6×NZB		
	2	44	28-84	2.3	M+F	14	Ath	NZB	NZB×SM	
		46	37-95	1.8	F (M?)	40	Chow	NOD	NOD×129S1	
		46	42-60	6.4	M (F?)	8	Chow	CAST	D2×CAST	
		60	32-100	2.5	M+F	10	Chow	NZW	B6×NZW	
		83	65-90	2.3	M (F?)	8	Chow	D2	B6×D2	
		83	78-88	4.1	F (M?)	18	Western	Het	B6×C3H-Apoe KO	
		83	74-103	2.8	M+F	11	Chow	B6	B6×CASA	
		84	2-102	2.2	F (M?)	68	Ath	D2	B6×D2	
		96	8-96	2.3	F (M?)	14	Ath	C3H	B6×C3H	
		100	22-100	2.4	F	10	Chow	RF	NZB×RF	
3		5	2-54	2.8	M+F	8	Chow	NZB	NZB×SM	
	5	2-26	3.0	M+F	24	Ath	NZB	NZB×SM	Add	
	17	13-79	2.1	M+F	16	Ath	PERA	PERA×I	Sex-specific	
	33	23-79	2.6	F (M?)	52	Chow	B6	B6×D2	Add	
	34	20-44	2.2	M (F?)	16	Ath	Het	129×RIII		
	42	2-52	3.0	M+F	14	Ath	NZB	NZB×SM		
	55	53-59	5.4	M	8	Chow	B6	B6×129		
	56	44-68	2.7	M (F?)	8	Chow	B6	B6×D2		
4	64	64-74	2.8	M+F	11	Chow	B6	B6×CASA		
	17	7-29	3.9	M	10	Chow	B6	B6×NOD	Sex-specific	
	21	11-31	4.3	M+F	16	Ath	PERA	D2×PERA	Ad	
	26	12-38	3.9	M+F	16	Ath	PERA	PERA×I	Ad	
	27	11-55	3.1	M (F?)	10	Chow	B6	B6×A		
	27	15-31	7.4	M (F?)	8	Chow	D2	D2×CAST		
	29	20-40	3.5	M (F?)	8	Chow	129	CAST×129S1		
	48	16-76	2.7	F	8	Chow	B6	B6×A		
	61	49-81	2.2	M (F?)	8	Chow	D2	B6×D2		
	62	54-68	3.7	F (M?)	68	Ath	B6	B6×D2		
5	6	3-11	6.3	M+F	16	Ath	PERA	PERA×I		
	10	3-49	4.3	M+F	16	Ath	129	B6×129		
	35	11-43	4.6	F (M?)	23	Ath	Het	(B6×NZB)B6		
	41	31-47	3.4	M (F?)	24	Chow	Het	(NON×NZO)NON		
	45	9-61	3.3	M+F	8	Chow	B6	B6×129		
	47	42-49	10.3	M+F	20	Ath	NZB	NZB×SM		
	47	21-49	8.7	M+F	24	Ath	NZB	NZB×SM		
	49	23-58	2.3	F (M?)	23	Ath	Het	B6×NZB		
	51	23-65	2.8	F (M?)	8	Chow	Het	B6×NZB		
	52	45-67	3.5	F (M?)	18	Ath	NZB	(NZB×SM)NZB		
	52	49-67	4.6	F (M?)	8	Chow	NZB	(NZB×SM)NZB		
	53	47-57	20	F	10	Chow	NZB	NZB×RF		
	59	41-61	10.6	M+F	14	Ath	NZB	NZB×SM		
	61	59-71	9.1	M+F	8	Chow	NZB	NZB×SM		
	65	51-80	2.2	F (M?)	18	Ath	NZB	(NZB×SM)NZB		
79	55-80	2.8	F (M?)	8	Chow	NZB	(NZB×SM)NZB			

TABLE 2. Continued.

Chr	Peak (cM)	Interval (cM)	LOD	Sex	Age (Weeks)	Diet	High	Cross	Remark	
6	29	16-67	2.3	M+F	10	Chow	NOD	B6×NOD	Add	
	33	20-46	2.7	M (F?)	8	Chow	D2	B6×D2	Add	
	46	34-78	2.1	M+F	16	Ath	PERA	PERA×I	Add	
	60	40-72	2.7	F (M?)	14	Ath	B6	B6×C3H	Add	
	70	58-76	4.0	M+F	8	Chow	NZB	NZB×SM		
	70	38-78	2.1	M+F	14	Ath	NZB	NZB×SM		
	72	48-78	4.4	M (F?)	8	Chow	CAST	D2×CAST		
	74	64-78	2.9	F (M?)	52	Chow	Het	B6×D2		
	78	2-78	2.4	F (M?)	20	Ath	B6	B6×129S1		
	7	9	9-76	2.2	M (F?)	8	Chow	Het	B6×A	
74		62-80	4.0	M	10	Chow	Het	B6×NOD	Sex-specific	
87		75-89	3.0	M+F	24	Ath	SM	NZB×SM	Add	
88		50-88	3.9	M+F	16	Ath	PERA	PERA×I		
8	2	2-34	2.7	F	10	Chow	NZB	NZB×RF		
	3	2-52	3.3	M+F	24	Ath	NZB	NZB×SM	Add	
	3	2-52	3.6	M+F	14	Ath	NZB	NZB×SM		
	36	26-44	6.1	M (F?)	10	Chow	B6	B6×A		
	38	24-46	4.6	F (M?)	8	Chow	B6	B6×A		
	46	34-66	2.3	F (M?)	20	Ath	129	B6×129S1		
	50	34-66	3.8	M+F	10	Chow	B6	B6×NOD		
	53	39-65	3.9	M+F	8	Chow	B6	B6×129S1		
	56	46-68	5.0	M (F?)	8	Chow	B6	B6×D2		
	73	3-76	4.3	M+F	11	Chow	B6	B6×CASA		
9	2	2-34	3.8	M	24	Ath	NZB	NZB×SM	Sex-specific	
	14	2-26	3.1	M (F?)	16	Ath	RIII	129×RIII	Add	
	18	18-25	8.1	M+F	11	Chow	CASA	B6×CASA		
	21	13-27	6.2	M+F	8	Chow	129	B6×129S1		
	22	6-34	3.0	F (M?)	20	Ath	129	B6×129		
	23	21-59	1.6	F (M?)	18	Ath	Het	NZB×SM		
	25	18-25	9.0	M+F	11	Chow	CASA	B6×CASA		
	25	22-50	6.4	F (M?)	40	Chow	Het	NOD×129		
	25	12-32	6.6	M (F?)	16	Ath	RIII	129×RIII		
	33	12-50	2.6	M+F	24	Ath	NZB	NZB×SM		
10	37	17-49	5.4	M+F	16	Ath	129	B6×129		
	2	2-66	2.4	M+F	10	Chow	Het	B6×NZW		
	63	53-72	3.2	F/M	8	Chow	NZB/ SM	NZB×SM	Sex-specific	
	68	39-68	2.2	M (F?)	10	Chow	B6	B6×A	Sex-specific	
	72	61-72	3.9	F	14	Ath	NZB	NZB×SM		
	11	18	14-66	2.7	M+F	14	Ath	Het	NZB×SM	
		27	17-43	2.7	M (F?)	10	Chow	B6	B6×A	Add
		30	18-54	3.4	M+F	16	Ath	PERA	PERA×I	Add
		36	14-50	3.4	M+F	16	Ath	PERA	D2×PERA	Add
		41	35-55	4.0	M+F	6	Chow	DU6i	D2×DU6i	
56		43-72	2.9	F (M?)	14	Ath	C3H	B6×C3H		
76		58-83	2.5	F (M?)	68	Ath	D2	B6×D2		
81		73-83	3.9	M+F	16	Ath	129	B6×129		
81		3-81	2.2	M+F	10	Chow	Het	B6×NZW		
12		10	6-44	3.4	F	10	Chow	NZB	NZB×RF	Sex-specific
	20	12-28	5.9	F (M?)	20	Ath	129	B6×129S1		
	28	10-40	4.8	M (F?)	16	Ath	RIII	129×RIII		
	30	17-45	7.4	M	8	Chow	I	PERA×I		
	38	12-54	2.1	M (F?)	8	Chow	B6	B6×D2		
	54	26-68	2.2	M+F	8	Chow	NZB	NZB×SM		
	56	10-74	2.8	M+F	20	Ath	NZB	NZB×SM		
	13	10	2-28	3.0	M+F	8	Chow	129	B6×129	Add
	14	19	15-29	3.1	M (F?)	8	Chow	B6	B6×D2	Add
		38	18-56	2.6	M+F	10	Chow	Het	B6×NOD	
15	16	4-34	2.6	F (M?)	14	Ath	B6	B6×C3H	Add	
	18	8-28	3.0	M (F?)	8	Chow	CAST	CAST×129		
16	23	15-35	3.5	F (M?)	8	Chow	B6	B6×A		
	38	37-54	2.6	M+F	8	Chow	NZB	NZB×SM		
	54	24-59	2.1	M+F	16	Ath	PERA	PERA×I		
	11	7-21	2.7	F (M?)	52	Chow	B6	B6×D2		
	22	20-28	2.6	F (M?)	18	Ath	Het	(NZB×SM)NZB		
	28	2-44	3.6	M+F	8	Chow	NZB	NZB×SM		
	40	24-50	2.4	M+F	24	Ath	NZB	NZB×SM		
	40	6-54	2.5	M+F	14	Ath	NZB	NZB×SM		
	49	32-49	1.6	F (M?)	18	Ath	NZB	(NZB×SM)NZB		
	58	3-58	2.1	M+F	16	Ath	PERA	PERA×I		

TABLE 2. Continued.

Chr	Peak (cM)	Interval (cM)	LOD	Sex	Age (Weeks)	Diet	High	Cross	Remark
17	9	5–31	2.2	F (M?)	20	Ath	B6	B6×129S1	
	12	8–61	2.4	M+F	6	Chow	D2	D2×DU6i	Sex-specific
	18	14–61	2.2	F	10	Chow	RF	NZB×RF	Add
	21	5–29	2.2	F (M?)	8	Chow	Het	B6×A	Add
	22	14–40	4.4	M	14	Ath	NZB	NZB×SM	
	22	22–50	1.7	F (M?)	18	Ath	NZB	(NZB×SM)NZB	
	28	8–42	2.4	M+F	8	Chow	NZB	NZB×SM	
	30	14–40	2.2	M+F	20	Ath	NZB	NZB×SM	
	30	14–40	2.8	M+F	24	Ath	NZB	NZB×SM	
	32	16–44	2.4	M+F	14	Ath	NZB	NZB×SM	
	39	31–51	2.6	M+F	16	Ath	D2	D2×PERA	
	53	39–55	2.3	M+F	16	Ath	I	PERA×I	
	58	40–60	2.8	F (M?)	18	wester	C3H	B6×C3H-Apoe KO	
	18	17	13–39	2.6	F (M?)	18	Wester	C3H	B6×C3H-Apoe KO
19		13–39	3.7	F (M?)	8	Chow	NZB	(NZB×SM)NZB	
26		10–42	2.1	M (F?)	8	Chow	CAST	D2×CAST	
28		15–45	2.7	M+F	8	Chow	129	B6×129	
30		16–48	2.5	M	10	Chow	B6	B6×A	
39		21–43	2.0	F (M?)	18	Ath	NZB	(NZB×SM)NZB	
39		11–58	3.0	M+F	8	Chow	NZB	NZB×SM	
53		41–58	3.0	F (M?)	14	Ath	C3H	B6×C3H	
55		39–58	2.8	F (M?)	52	Chow	D2	B6×D2	
58		41–58	2.8	M+F	14	Ath	NZB	NZB×SM	
58		7–58	4.0	M+F	20	Ath	NZB	NZB×SM	
19	3	3–57	1.9	F (M?)	40	Chow	Het	NOD×129	Sex-specific
	14	6–52	2.4	F (M?)	8	Chow	B6	B6×A	
	34	26–56	3.2	F	20	Ath	NZB	NZB×SM	
	34	24–54	2.6	M+F	10	Chow	NZW	B6×NZW	
	36	20–56	2.9	M+F	14	Ath	NZB	NZB×SM	
	49	35–50	5.6	F	10	Chow	NZB	NZB×RF	
	56	18–56	2.2	M+F	8	Chow	NZB	NZB×SM	
	56	38–56	3.0	M+F	20	Ath	NZB	NZB×SM	
	56	28–56	3.0	M+F	24	Ath	NZB	NZB×SM	

Ath, atherogenic; KO, knockout.

a region containing 343 genes with assigned MGI IDs (<http://www.informatics.jax.org>), as determined using the Biomart tool available from the Ensembl genome database [<http://www.ensembl.org/index.html>, Ensembl Genes 69 dataset:Mus musculus genes (GRCm38)]. The raw centimorgan positions for the confidence interval were converted to genome coordinates (NCBI, Bld37) using the Mouse Map Converter tool (<http://cgd.jax.org>). We then examined this interval to identify SNPs that met the following allele conditions:

$$(PERA = B6 = D2 = 129) \neq (I = A = CAST) \text{ (Eq. 1)}$$

The SNP dataset used for this analysis was the CGD-MDA1 dataset, which is publically available (<http://phenome.jax.org>); all SNP in the above QTL interval in this database were examined. While this SNP dataset does not contain all known mouse SNP, it is the most complete, publically available SNP dataset containing data for all of the strains listed in Equation 1. Another limitation is that we excluded all SNPs that did not have complete genotype information for our strains of interest. Therefore, until complete genome sequences for all involved strains is available, we cannot exclude the possibility that candidate genes are missed. Of the 3,483 SNP for which data was available for the minimal QTL interval, only 8 SNPs met the allele distribution pattern defined by Equation 1. These SNP were all located in a narrow region between

49.86 and 50.58 Mb. This narrow region does not contain the coding region for any gene. However, the most proximal of the SNPs is located 937 bp distal to the start codon for the *Grin3a* gene. The *Grin3a* gene runs on the negative strand, and our SNPs overlap with its predicted regulatory/promoter region. There are no polymorphisms in the coding region of *Grin3a* that match the strain pattern shown in Equation 1.

Identification of *Etv6* as a candidate gene for an HDL QTL on distal mouse Chr 6

On the distal end of Chr 6, we identified a cluster of three comapping QTL with peak locations between 70 and 74 cM (Table 2, Fig. 3B). These QTL were mapped in the following crosses (underlined strains have the high allele): SM×NZB (peak at 70 cM), D2×CAST (peak at 72 cM), and B6×D2 (peak at 74 cM). The B6×D2 QTL was only a suggestive QTL, and the allele effects for this QTL were not conclusive. Very few mice were phenotyped in the B6×D2 cross, severely underpowering the mapping in this study. However, the D2 strain was used in another cross with a QTL mapping to this location, suggesting that this B6×D2 QTL is valid. Using methods similar to that which was used for the Chr 4 locus, we then attempted to narrow this QTL to a single candidate gene. The minimum shared interval for this cluster on distal Chr 6 extended from 64 to 76 cM (131.92–143.65 Mb). This relatively gene-dense region contains 124 known or predicted genes. Using SNP comparison

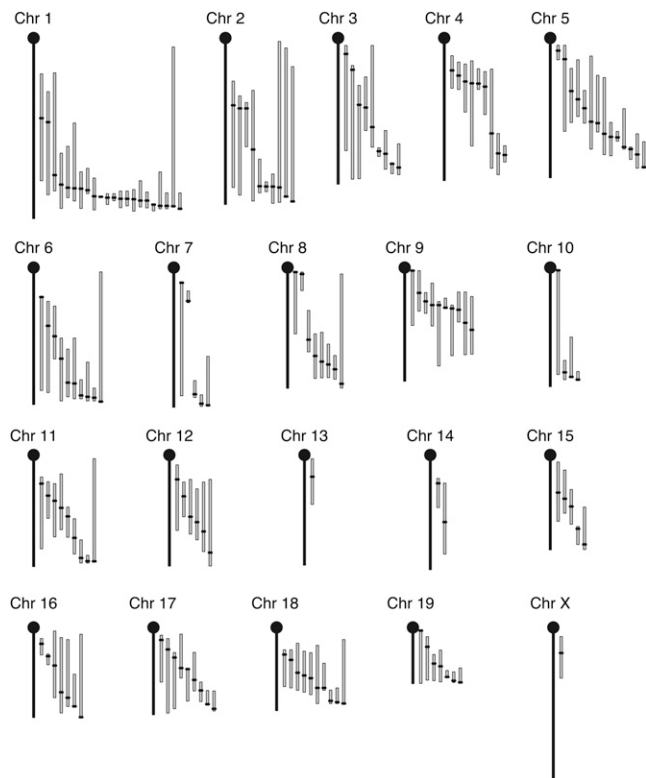


Fig. 1. Mouse chromosome map with the recalculated HDL QTL. Each bar represents the 95% confidence interval, with the black dot indicating the peak position of the QTL.

such that the conditions in Equation 2 were met, we were able to narrow this QTL to a single region spanning from 134.00 to 134.09 Mb.

$$(SM = D2) \neq (NZB = CAST = B6) \quad (Eq. 2)$$

This region contains a single gene, *Etv6*. No polymorphisms are found in the coding region of *Etv6* that match the strain pattern shown in Equation 2. This gene appears to be moderately expressed in the liver (20). Therefore, we examined the expression pattern for this gene in our previously published liver expression strain survey (21) using the reported Q values (<http://cgd.jax.org/datasets/expression/10strain.shtml>), but it did not show differential expression between strains in the three crosses defining this QTL. Thus, it appears that this gene either does not function directly in the liver to modulate HDL or that the causative mutation(s) in this gene do not affect transcription levels but may still influence protein levels (22).

Cluster of QTL on distal Chr 19 can be narrowed to a small number of candidate genes

The new QTL map for Chr 19 differs significantly from the previous map (Fig. 3C). In addition to shifts in the peaks of QTL identified in several crosses, we identified several new peaks in other crosses but could not find some of the peaks reported in the literature. We did identify an interesting cluster of three QTL at the distal end of Chr 19 in the following crosses (underlined strains have the high

allele): NZB×RF (peak at 49 cM), NZW×B6 (peak at 54 cM), and NZB×SM (peak at 56 cM). The last marker genotyped in the NZB×RF cross is located at 50 cM. The LOD score at this marker is nearly identical to the LOD score at the location of peak association. Thus, while the proximal boundary of the confidence interval for this QTL can be determined, the distal boundary cannot. By using the distal limit of the confidence interval for the B6×NZW cross, we determined that the narrowest common region for this QTL extends from 42 to 56 cM (48.5–59.5 Mb). As for the other QTL clusters described above, we used SNP comparison to narrow the list of candidate genes. The conditions for the comparison were:

$$(NZB = NZW) \neq (RF = B6 = SM) \quad (Eq. 3)$$

Unlike the two previous QTL clusters, we were unable to narrow this QTL to a single candidate gene. Fifteen known genes (*Sorcs3*, *Sorcs1*, *Add3*, *Mxi1*, *5830416P10Rik*, *Rbm20*, *Pdcd4*, *Shoc2*, *Acl5*, *Vti1a*, *Tcf7l2*, *B230217012Rik*, *Fam160b1*, *Trub1*, and *Atrnl1*) and two predicted genes (*1700001K23Rik* and *Gm16745*) were identified as containing at least one SNP for which the alleles met the conditions defined in Equation 3.

To further narrow the list of genes for this QTL, we examined liver expression for strains included in our previously published gene expression strain survey (21). While liver expression data are not available for two of the strains used to map QTL identified in this cluster (NZW and RF), data are available for NZB, B6, and SM. Statistically significant differential expression was noted for *Add3*, *Shoc2*, and *Fam160b1*, and nearly statistically significant differential expression was noted for *Rbm20*. The differential expression profile for *Fam160b1*, *Rbm20*, and *Shoc2* showed the expected profile such that the two low allele strains (B6 and SM) were expressed at levels different than that for the high allele NZB strain, but expression was not different when comparing B6 with SM. The expression profile for the *Add3* gene did not follow this pattern, as expression was not different when comparing the high allele NZB strain to the low allele B6 strain.

As coding region polymorphisms can affect gene function in a way that is not necessarily reflected in expression profiles, we looked for coding region polymorphisms (nonsynonymous, nonsense) and splice site SNPs in which the allele pattern met the requirements defined in Equation 3; none were found, however, in the SNP databases available for these five strains. We then examined the Sanger resequencing databases to find any known nonsynonymous (Cn) SNPs in our 15 candidate genes in the classical inbred strains (i.e., not wild derived). Of the five strains of interest for this QTL cluster, only B6 has been resequenced to date. Nevertheless, given the number of strains that are resequenced, examination of this database should give a more complete listing of Cn SNP than other available databases. Nonsynonymous SNPs are listed in the Sanger database in *Add3*, *Rbm20*, *Sorcs3*, *Sorcs1*, *Fam160b1*, *Atrnl1*, and *Trub1*. The only Cn SNP listed in *Add3* appeared to be private to the NON/ShiLj strain,

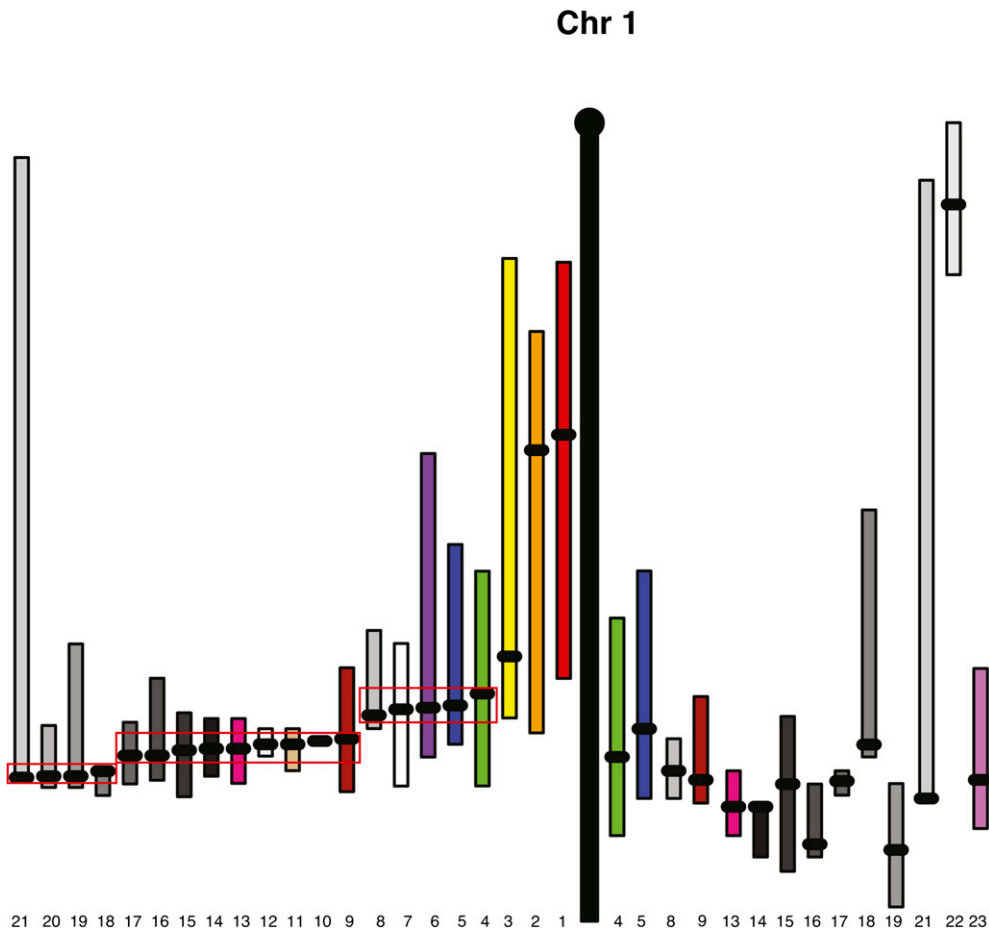


Fig. 2. Chromosome 1 with the old map positions on the right and the new QTL map positions on the left. Each bar represents the confidence interval of a QTL within a cross, with the black dot indicating the peak. Bars with the same number on the left and right are the QTL in the same cross. Careful examination of the QTL mapped to distal Chr 1 in this study shows three discrete clusters of comapping QTL: one cluster of five QTL centered at 70 cM, one cluster of nine QTL centered at 80 cM, and one cluster of four QTL centered at 85 cM.

and the only two in *Rbm20* appeared to be private to the C57BL substrains (C57BL/6J and C57BL/6NJ). We then used the SIFT tool (<http://sift.jcvi.org/>) to determine whether the resulting amino acid changes for the remaining Cn SNPs were predicted to have a functional consequence(s). We found one such Cn SNP (*rs37375751*) in the *Sorcs3* gene, but this SNP was not predicted to affect protein function. Four Cn SNPs are listed in the *Sorcs1* gene in the classical inbred strains. One SNP (at 50255976 Mb, no rs number available, NCBI, Bld37) appeared to be a private SNP in the AKR/J strain. Two others, *rs37453589* and a SNP at 50752804 Mb (no rs number available), were predicted to be tolerated. A fourth SNP in this gene, at 50752876 Mb (no rs number available), was predicted to result in an A-to-V substitution. This substitution was predicted not to be tolerated and thus had the potential to impact protein function. While this SNP appears quite polymorphic among inbred strains, the alanine amino acid at this location is quite conserved among other mammals. We resequenced this SNP in the five strains of interest for this QTL cluster and determined that the genotypes for the five strains fit Equation 3. Five Cn SNPs are listed

in the *Fam160b1* gene, for the classical inbred strains (*rs36742147*, *rs31128381*, *rs38343270*, *rs37035338*, and *rs36675440*). However, none of these SNPs is predicted to affect protein function. Likewise, a single Cn SNP is listed in the *Atrn11* gene (*rs36943069*), but again this SNP is expected to be tolerated with regard to protein function. A single Cn SNP is listed in the *Trub1* gene. This SNP at 57532595 Mb (no rs number available), results in a change from S to F at amino acid position 40, which is predicted not to be tolerated with regard to protein function. While serine at this position is well conserved among mammals, a phenylalanine is found at this position in opossums. A number of strains are polymorphic for this SNP, including the NZO/HILtJ strain, a close relative of the NZB/BINJ strain. We then resequenced this SNP in the five strains of interest for this QTL cluster and determined that the genotypes for the five strains fit Equation 3. In sum, the expression data provide support for *Fam160b1*, *Shoc2*, and *Rbm20*, and the presence of Cn SNPs provide support for *Sorcs1* and *Trub1* as candidates for this Chr 19 QTL. Further work will be required to further narrow this QTL.

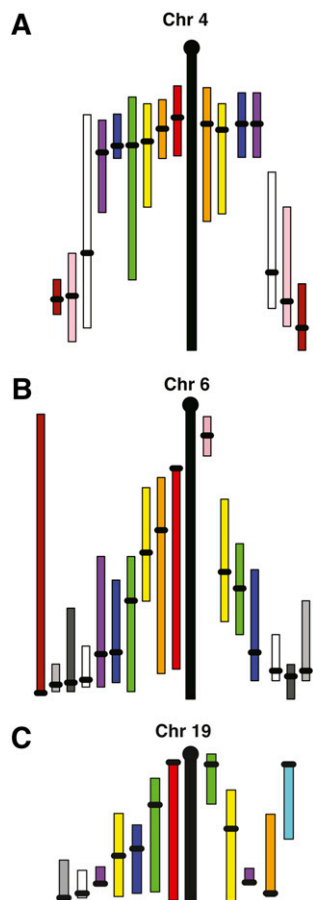


Fig. 3. Chromosomes 4 (A), 6 (B), and 19 (C) with the old map positions on the right and the new QTL map positions on the left. Each bar represents the confidence interval of a QTL within a cross, with the black dot indicating the peak. Bars with the same color on the left and right are QTL in the same cross.

DISCUSSION

QTL analysis is a reliable method to identify loci involved in the variation of a phenotype of interest, and since the key publication by Lander and Botstein (23), thousands of QTL studies have been performed for many different phenotypes and utilizing different species. A disadvantage of the method is the low resolution of mapping, as it is dependent on the number of recombinations in the population, which is inherently low in a two-generation cross between inbred strains. Because of this low resolution, a typical QTL spans 10–20 cM and contains hundreds of genes. We and others have developed statistical approaches that combine the data from multiple crosses to increase mapping resolution yielding narrower QTL intervals and bioinformatics methods, such as haplotyping, that allow to decrease the number of possible candidate genes within an interval (10). Using these methods, either in isolation or in combination, has allowed for the identification of causative genes for QTLs. However, these approaches strongly depend on accurate QTL mapping, and inclusion of an inaccurately mapped QTL or exclusion of an accurately mapped QTL can lead to false conclusions.


The literature reports a number of clusters of putatively comapping HDL QTL for which no candidate gene has been identified. For many of these clusters, our analysis suggests the existence of additional comapping QTL (i.e., an addition of QTL to a locus) or inappropriate conclusions regarding comapping (i.e., the eliminated QTL from a locus). In the first situation, the addition of a QTL can provide additional haplotypes, which might allow for further narrowing of the interval. In the second situation, candidate genes may have been inappropriately eliminated by using the “false” strains that were included in the haplotype comparison.

The advantages of our reanalysis are demonstrated in the three examples presented above. In the first example highlighting a QTL on Chr 4, we were able to narrow the interval to one single gene, Glutamate receptor ionotropic NMDA3A (*Grin3a*). *Grin3a*, which is also known as NR3A, codes for an inhibitory subunit of NMDA-type glutamate receptors. Traditional NMDA receptors are key players in glutamate-facilitated neurotransmission (24). Studies have suggested that expression of *Grin3a* is highest in selected regions of the brain in the postnatal period and in the adult retina, where the GRIN3A/NR3A subunit is thought to inhibit NMDA receptor Ca^{2+} permeability and has a neuroprotective function (25). Similarly, expression of *Grin3a* is high in the neonatal kidney, but expression does persist into adulthood. As in the brain, *Grin3a* appears to serve a protective role for the cells of the collecting duct of the kidney (26). While mechanism by which *Grin3a* influences HDL levels remains unknown, this gene was recently identified to be associated with HDL in a human genome-wide association study (27).

In the second example, for a Chr 6 QTL, we were also able to narrow the interval to a single gene (*Etv6*) using the QTL data. *Etv6* is an ubiquitously expressed gene encoding a transcription repressor, and ETV6 is a member of the ETS family of transcription factors (28). Most studies on ETV6 have focused on the fusion proteins that can arise from chromosomal rearrangements between *Etv6* and other genes encoding transcription factors, such as *Runx1*, and which have been implicated as being causative in some forms of leukemia (29). While the mechanism by which ETV6 regulates HDL levels is unclear, studies of gene networks associated with ETV6 action have suggested that this transcription repressor regulates genes associated with cholesterol biogenesis (30).

Finally, in our third example, Chr 19, combining the newly calculated QTL narrowed the region to a cluster of 15 genes, for which additional evidence exists supporting 5 as candidates for this QTL. This QTL is different from the other two examples, as it seems to be exclusive to NZ strains. Both the NZB/B1NJ and the NZW/LacJ strains can be traced back to a common set of mice brought to Australia in the 1930s, and recent analysis of the relatedness of inbred strains shows that the NZW/LacJ and the NZB/B1NJ strains are indeed genetically very closely related (31). In all three crosses contributing to the QTL cluster on distal Chr 19, one of the NZ strains was the high allele, suggesting that the alleles underlying this QTL are

private to the NZ strains. As the modern NZO/H1L_TJ is related to both the NZW/LacJ and the NZB/BNJ strains, it is possible that this strain also carries the private “NZ” allele at this locus. The addition of the NZO/H1L_TJ strain to the haplotyping for this locus does eliminate the *Add3*, *170001K23Rik*, *Mxi11*, and *Tcf7l2* genes. Future work must be conducted, however, to determine whether this QTL is indeed caused by private NZ alleles. The 5 candidate genes for this QTL are *Fam160b1*, *Shoc2*, *Rbm20*, *Sorcs1*, and *Trub1*. Of these 5, *Sorcs1* is the most likely candidate gene based on the existing evidence. This gene codes for a Vsp10p-D receptor family member transmembrane protein, which functions to sort and traffic proteins (32). Genetic variation in this gene has been associated with both the development of type II diabetes (33, 34) and risk for development of Alzheimer disease (35). These two diseases are correlated with serum lipid levels and genetic variation in another Vsp10p-D receptor gene, *Sort1*, which has been linked to serum LDL levels (36, 37). The remaining 4 genes have been poorly studied, and thus it is unclear how or whether these genes could function to modulate serum HDL levels. Mutations in *SHOC2* can cause Noonan syndrome, an autosomal dominant disorder characterized by short stature, down-slanted eyes, cardiovascular defects, and increased tumor risks (38). The *Rbm20* gene codes for RNA binding protein/RNA splicing protein, which shows particularly high expression in muscle, heart, and brain, and recent studies have shown that null mutations in this gene are associated with hereditary cardiomyopathies (39). Little is known about *Trub1*; it has been identified as a tRNA pseudouridination gene.

In conclusion, our reanalysis of the QTL data for 23 crosses results in an improved map for HDL QTL and facilitates the identification of HDL genes in the mouse. We show that using this approach, we can identify previously missed QTL and locate QTL on different regions of a chromosome. The new HDL QTL map allows for reliable combining of QTL data and candidate gene analysis, which we demonstrate by identifying *Grin3a*, *Etv6*, and a cluster of five genes as likely candidate genes for QTL on Chr 4, 6, and 19, respectively. 

REFERENCES

- Brewer, H. B. 2004. High-density lipoproteins: a new potential therapeutic target for the prevention of cardiovascular disease. *Arterioscler. Thromb. Vasc. Biol.* **24**: 387–391.
- Gordon, T., W. P. Castelli, M. C. Hjortland, W. B. Kannel, and T. R. Dawber. 1977. High density lipoprotein as a protective factor against coronary heart disease. The Framingham Study. *Am. J. Med.* **62**: 707–714.
- Castelli, W. P., R. J. Garrison, P. W. Wilson, R. D. Abbott, S. Kalousdian, and W. B. Kannel. 1986. Incidence of coronary heart disease and lipoprotein cholesterol levels. The Framingham Study. *JAMA.* **256**: 2835–2838.
- Assmann, G., H. Schulte, A. von Eckardstein, and Y. Huang. 1996. High-density lipoprotein cholesterol as a predictor of coronary heart disease risk. The PROCAM experience and pathophysiological implications for reverse cholesterol transport. *Atherosclerosis.* **124(Suppl.)**: S11–S20.
- Sharrett, A. R., C. M. Ballantyne, S. A. Coady, G. Heiss, P. D. Sorlie, D. Catellier, and W. Patsch, Atherosclerosis Risk in Communities Study Group. 2001. Coronary heart disease prediction from lipoprotein cholesterol levels, triglycerides, lipoprotein(a), apolipoproteins A-I and B, and HDL density subfractions: The Atherosclerosis Risk in Communities (ARIC) Study. *Circulation.* **104**: 1108–1113.
- Wang, X., and B. Paigen. 2002. Quantitative trait loci and candidate genes regulating HDL cholesterol: a murine chromosome map. *Arterioscler. Thromb. Vasc. Biol.* **22**: 1390–1401.
- Wang, X., and B. Paigen. 2005. Genetics of variation in HDL cholesterol in humans and mice. *Circ. Res.* **96**: 27–42.
- Ackert-Bicknell, C. L., D. Karasik, Q. Li, R. V. Smith, Y-H. Hsu, G. A. Churchill, B. J. Paigen, and S-W. Tsaih. 2010. Mouse BMD quantitative trait loci show improved concordance with human genome-wide association loci when recalculated on a new, common mouse genetic map. *J. Bone Miner. Res.* **25**: 1808–1820.
- Ridgway, W. M., B. Healy, L. J. Smink, D. Rainbow, and L. S. Wicker. 2007. New tools for defining the “genetic background” of inbred mouse strains. *Nat. Immunol.* **8**: 669–673.
- DiPetrillo, K., X. Wang, I. M. Stylianou, and B. Paigen. 2005. Bioinformatics toolbox for narrowing rodent quantitative trait loci. *Trends Genet.* **21**: 683–692.
- Blake, J. A., J. E. Richardson, M. T. Davisson, and J. T. Eppig. 1997. The Mouse Genome Database (MGD). A comprehensive public resource of genetic, phenotypic and genomic data. The Mouse Genome Informatics Group. *Nucleic Acids Res.* **25**: 85–91.
- Broman, K. W., and S. Sen. 2009. A Guide to QTL Mapping with R/qtl. Springer, New York.
- Shifman, S., J. T. Bell, R. R. Copley, M. S. Taylor, R. W. Williams, R. Mott, and J. Flint. 2006. A high-resolution single nucleotide polymorphism genetic map of the mouse genome. *PLoS Biol.* **4**: e395.
- Cox, A., C. L. Ackert-Bicknell, B. L. Dumont, Y. Ding, J. T. Bell, G. A. Brockmann, J. E. Wergedal, C. J. Bult, B. Paigen, J. Flint, et al. 2009. A new standard genetic map for the laboratory mouse. *Genetics.* **182**: 1335–1344.
- Sehayek, E., E. M. Duncan, H. J. Yu, L. Petukhova, and J. L. Breslow. 2003. Loci controlling plasma non-HDL and HDL cholesterol levels in a C57BL/6J x CASA/Rk intercross. *J. Lipid Res.* **44**: 1744–1750.
- Colinayo, V. V., J-H. Qiao, X. Wang, K. L. Krass, E. Schadt, A. J. Lusis, and T. A. Drake. 2003. Genetic loci for diet-induced atherosclerotic lesions and plasma lipids in mice. *Mamm. Genome.* **14**: 464–471.
- Wang, X., R. Korstanje, D. Higgins, and B. Paigen. 2004. Haplotype analysis in multiple crosses to identify a QTL gene. *Genome Res.* **14**: 1767–1772.
- Su, Z., A. Cox, Y. Shen, I. M. Stylianou, and B. Paigen. 2009. Farp2 and Stk25 are candidate genes for the HDL cholesterol locus on mouse chromosome 1. *Arterioscler. Thromb. Vasc. Biol.* **29**: 107–113.
- Su, Z., X. Wang, S-W. Tsaih, A. Zhang, A. Cox, S. Sheehan, and B. Paigen. 2009. Genetic basis of HDL variation in 129/SvImJ and C57BL/6J mice: importance of testing candidate genes in targeted mutant mice. *J. Lipid Res.* **50**: 116–125.
- Visel, A., C. Thaller, and G. Eichele. 2004. GenePaint.org: an atlas of gene expression patterns in the mouse embryo. *Nucleic Acids Res.* **32**: D552–D556.
- Shockley, K. R., D. Witmer, S. L. Burgess-Herbert, B. Paigen, and G. A. Churchill. 2009. Effects of atherogenic diet on hepatic gene expression across mouse strains. *Physiol. Genomics.* **39**: 172–182.
- Ghazalpour, A., B. Bennett, V. A. Petyuk, L. Orozco, R. Hagopian, I. N. Mungrue, C. R. Farber, J. Sinsheimer, H. M. Kang, N. Furlotte, et al. 2011. Comparative analysis of proteome and transcriptome variation in mouse. *PLoS Genet.* **7**: e1001393.
- Lander, E. S., and D. Botstein. 1989. Mapping mendelian factors underlying quantitative traits using RFLP linkage maps. *Genetics.* **121**: 185–199.
- Fitzgerald, P. J. 2012. The NMDA receptor may participate in widespread suppression of circuit level neural activity, in addition to a similarly prominent role in circuit level activation. *Behav. Brain Res.* **230**: 291–298.
- Nakanishi, N., S. Tu, Y. Shin, J. Cui, T. Kurokawa, D. Zhang, H-S. V. Chen, G. Tong, and S. A. Lipton. 2009. Neuroprotection by the NR3A subunit of the NMDA receptor. *J. Neurosci.* **29**: 5260–5265.
- Sproul, A., S. L. Steele, T. L. Thai, S. Yu, J. D. Klein, J. M. Sands, and P. D. Bell. 2011. N-methyl-D-aspartate receptor subunit NR3a expression and function in principal cells of the collecting duct. *Am. J. Physiol. Renal Physiol.* **301**: F44–F54.
- Willer, C. J., S. Sanna, A. U. Jackson, A. Scuteri, L. L. Bonnycastle, R. Clarke, S. C. Heath, N. J. Timpson, S. S. Najjar, H. M. Stringham, et al. 2008. Newly identified loci that influence lipid concentrations and risk of coronary artery disease. *Nat. Genet.* **40**: 161–169.
- Coyne, H. J., S. De, M. Okon, S. M. Green, N. Bhachech, B. J. Graves, and L. P. McIntosh. 2012. Autoinhibition of ETV6 (TEL)

- DNA binding: appended helices sterically block the ETS domain. *J. Mol. Biol.* **421**: 67–84.
29. Bohlander, S. K. 2005. ETV6: a versatile player in leukemogenesis. *Semin. Cancer Biol.* **15**: 162–174.
 30. Boily, G., P. Beaulieu, J. Healy, and D. Sinnett. 2008. Connections between ETV6-modulated genes: identification of shared features. *Cancer Inform.* **6**: 183–201.
 31. Petkov, P. M., J. H. Graber, G. A. Churchill, K. Dipetrillo, B. L. King, and K. Paigen. 2005. Evidence of a large-scale functional organization of mammalian chromosomes. *PLoS Genet.* **1**: e33.
 32. Nielsen, M. S., S. J. Keat, J. W. Hamati, P. Madsen, J. J. Gutzmann, A. Engelsberg, K. M. Pedersen, C. Gustafsen, A. Nykjaer, J. Gliemann, et al. 2008. Different motifs regulate trafficking of SorCS1 isoforms. *Traffic.* **9**: 980–994.
 33. Goodarzi, M. O., D. M. Lehman, K. D. Taylor, X. Guo, J. Cui, M. J. Quiñones, S. M. Clee, B. S. Yandell, J. Blangero, W. A. Hsueh, et al. 2007. SORCS1: a novel human type 2 diabetes susceptibility gene suggested by the mouse. *Diabetes.* **56**: 1922–1929.
 34. Clee, S. M., B. S. Yandell, K. M. Schueler, M. E. Rabaglia, O. C. Richards, S. M. Raines, E. A. Kabara, D. M. Klass, E. T-K. Mui, D. S. Stapleton, et al. 2006. Positional cloning of Sorcs1, a type 2 diabetes quantitative trait locus. *Nat. Genet.* **38**: 688–693.
 35. Reitz, C., S. Tokuhiro, L. N. Clark, C. Conrad, J-P. Vonsattel, L-N. Hazrati, A. Palotás, R. Lantigua, M. Medrano, I. Z. Jiménez-Velázquez, et al. 2011. SORCS1 alters amyloid precursor protein processing and variants may increase Alzheimer's disease risk. *Ann. Neurol.* **69**: 47–64.
 36. Shirts, B. H., S. J. Hasstedt, K. N. Hopkins, and S. C. Hunt. 2011. Evaluation of the gene-age interactions in HDL cholesterol, LDL cholesterol, and triglyceride levels: the impact of the SORT1 polymorphism on LDL cholesterol levels is age dependent. *Atherosclerosis.* **217**: 139–141.
 37. Willer, C. J., and K. L. Mohlke. 2012. Finding genes and variants for lipid levels after genome-wide association analysis. *Curr. Opin. Lipidol.* **23**: 98–103.
 38. Denayer, E., H. Peeters, L. Sevenants, M. Derbent, J. P. Fryns, and E. Legius. 2012. NRAS Mutations in Noonan Syndrome. *Mol Syndromol.* **3**: 34–38.
 39. Guo, W., S. Schafer, M. L. Greaser, M. H. Radke, M. Liss, T. Govindarajan, H. Maatz, H. Schulz, S. Li, A. M. Parrish, et al. 2012. RBM20, a gene for hereditary cardiomyopathy, regulates titin splicing. *Nat. Med.* **18**: 766–773.
 40. Pitman, W. A., R. Korstanje, G. A. Churchill, E. Nicodeme, J. J. Albers, M. C. Cheung, M. A. Staton, S. S. Sampson, S. Harris, and B. Paigen. 2002. Quantitative trait locus mapping of genes that regulate HDL cholesterol in SM/J and NZB/B1NJ inbred mice. *Physiol. Genomics.* **9**: 93–102.
 41. Lyons, M. A., H. Wittenburg, R. Li, K. A. Walsh, G. A. Churchill, M. C. Carey, and B. Paigen. 2003. Quantitative trait loci that determine lipoprotein cholesterol levels in DBA/2J and CAST/Ei inbred mice. *J. Lipid Res.* **44**: 953–967.
 42. Wang, X., I. Le Roy, E. Nicodeme, R. Li, R. Wagner, C. Petros, G. A. Churchill, S. Harris, A. Darvasi, J. Kirilovsky, et al. 2003. Using advanced intercross lines for high-resolution mapping of HDL cholesterol quantitative trait loci. *Genome Res.* **13**: 1654–1664.
 43. Korstanje, R., R. Li, T. Howard, P. Kelmenson, J. Marshall, B. Paigen, and G. Churchill. 2004. Influence of sex and diet on quantitative trait loci for HDL cholesterol levels in an SM/J by NZB/B1NJ intercross population. *J. Lipid Res.* **45**: 881–888.
 44. Ishimori, N., R. Li, P. M. Kelmenson, R. Korstanje, K. A. Walsh, G. A. Churchill, K. Forsman-Semb, and B. Paigen. 2004. Quantitative trait loci analysis for plasma HDL-cholesterol concentrations and atherosclerosis susceptibility between inbred mouse strains C57BL/6J and 129S1/SvImJ. *Arterioscler. Thromb. Vasc. Biol.* **24**: 161–166.
 45. Lyons, M. A. 2004. Quantitative trait loci that determine lipoprotein cholesterol levels in an intercross of 129S1/SvImJ and CAST/Ei inbred mice. *Physiol. Genomics.* **17**: 60–68.
 46. Lyons, M. A. 2004. Genetic contributors to lipoprotein cholesterol levels in an intercross of 129S1/SvImJ and RIIS/J inbred mice. *Physiol. Genomics.* **17**: 114–121.
 47. Wittenburg, H., M. A. Lyons, R. Li, U. Kurtz, X. Wang, J. Mössner, G. A. Churchill, M. C. Carey, and B. Paigen. 2006. QTL mapping for genetic determinants of lipoprotein cholesterol levels in combined crosses of inbred mouse strains. *J. Lipid Res.* **47**: 1780–1790.
 48. Stylianou, I. M., S-W. Tsaih, K. Dipetrillo, N. Ishimori, R. Li, B. Paigen, and G. A. Churchill. 2006. Complex genetic architecture revealed by analysis of high-density lipoprotein cholesterol in chromosome substitution strains and F2 crosses. *Genetics.* **174**: 999–1007.
 49. Wergedal, J. E., C. L. Ackert-Bicknell, W. G. Beamer, S. Mohan, D. J. Baylink, and A. K. Srivastava. 2007. Mapping genetic loci that regulate lipid levels in a NZB/B1NJxRF/J intercross and a combined intercross involving NZB/B1NJ, RF/J, MRL/MpJ, and SJL/J mouse strains. *J. Lipid Res.* **48**: 1724–1734.
 50. Brockmann, G. A., E. Karatayli, C. Neuschl, I. M. Stylianou, S. Aksu, A. Ludwig, U. Renne, C. S. Haley, and S. Knott. 2007. Genetic control of lipids in the mouse cross DU6i x DBA/2. *Mamm. Genome.* **18**: 757–766.
 51. Li, Q., Y. Li, Z. Zhang, T. R. Gilbert, A. H. Matsumoto, S. E. Dobrin, and W. Shi. 2008. Quantitative trait locus analysis of carotid atherosclerosis in an intercross between C57BL/6 and C3H apolipoprotein E-deficient mice. *Stroke.* **39**: 166–173.
 52. Su, Z., N. Ishimori, Y. Chen, E. H. Leiter, G. A. Churchill, B. Paigen, and I. M. Stylianou. 2009. Four additional mouse crosses improve the lipid QTL landscape and identify Lipg as a QTL gene. *J. Lipid Res.* **50**: 2083–2094.
 53. Leiter, E. H., P. C. Reifsnyder, R. Wallace, R. Li, B. King, and G. C. Churchill. 2009. NOD x 129.H2(g7) backcross delineates 129S1/SvImJ-derived genomic regions modulating type 1 diabetes development in mice. *Diabetes.* **58**: 1700–1703.